Journal of
Ship&Ocean
Technology
©MARCH 2005

SOTECH Vol. 9, No. 1, pp. 11~26, 2005

Dynamic Analysis of Multiple-Body Floating Platforms Coupled with Mooring Lines and Risers

Young-Bok Kim[1] and Moo- Hyun Kim[2]

[1] Marine Research Institute, Samsung Heavy Industry, Co. Ltd., Kyeongnam, Korea;
E-mail: yb09.kim @samsung.com
[2] Civil Engineering, Department, Texas A&M University, Texas, U.S.A.

Abstract

In this study, the program to investigate the multiple body interaction effects between a floating platform and a shuttle tanker considering the coupled effect of hull (FPSO) with mooring lines and risers was developed. The coupled analysis program, which is called WINPOST-MULT using the hydrodynamic analysis results by WAMIT, was made. For the verification of WINPOST-MULT by means of numerical experiments, two multiple-body models of an FPSO-FPSO and an FPSO-shuttle tanker system are adopted.

With the FPSO-FPSO model and a two-mass-spring system to idealize two identical bodies for the 100-year storm wave condition in GOM, the numerical simulations were performed to investigate the interaction effects between two identical bodies. For the more reality, the coupled analysis for the FPSO-shuttle tanker model in the tandem arrangement was carried out in the consideration of the environmental condition of the West Africa Sea as a rather mild condition. Through the case studies with interaction effect and without interaction effect by the iteration method and the combined method, it is verified that the program is a very useful tool for the analysis of the interaction problem of multiple-body system and the coupled problem of the hull/mooring/riser.

Keywords: multiple-body floating platform, hydrodynamic interaction effect, hull/mooring/riser coupled analysis, 100-year storm condition in GOM, environmental condition in West Africa sea, MMS

1 Introduction

Recently, floating structures have been invented and their installation has been attempted worldwide because of cost effectiveness, in an attempt to replace traditional fixed jacket platforms. These structures include the ship-shaped vessel called an FPSO(Floating Production Storage and Offloading Unit), the column stabilized semi-submergible platform, the spar platform, and the tension leg platform(TLP). The last two types have been designed and installed in the Gulf of Mexico(GOM) for the last decade. The recent trend in the installation of floating structures shows the water depth getting deeper and deeper since the oil and gas fields are expedited and discovered in the deeper sea. This means the more developed designs should be invented and studied realistically for the installation of the floating structures in deep water of 6,000 ft or more. Floating structures are more attractive to the industrial companies because they can allow for environmental conditions more flexibly than the fixed structures.

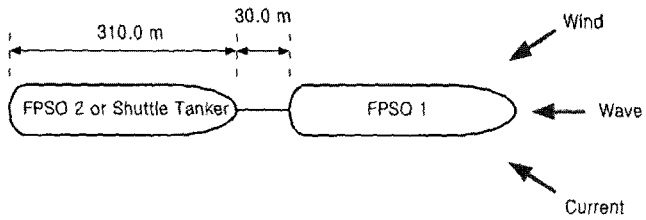

Figure 1: Configuration of the mooring systems (Tandem mooring system)

For the floating structures in deep water, many researchers have proved that coupled dynamic analyses are indispensable to get more convincing results from the platform responses and the line tensions than those of conventional uncoupled analysis methods (Pauling and Webster 1986, Kim et al 1994, Ran and Kim 1997, Ran et al 1999, Ma et al 2000). Since the ship-shaped floating structures called FPSOs have more advantages as the solutions to comparably large deck space, cost-saving problems and less risk of oil spills, they will have to be potentially attractive production systems in ultra deep water of the GOM. Nowadays, the Mineral Management System (MMS) has approved the installation of an FPSO under the condition that the vessel has the construction of a double hull tanker in the GOM. The large storage capacity is the biggest advantage because no pipeline has to be laid out from the sea floor to the land. A kind of LNG carrier or oil shuttle tanker is substituted for the pipelines for the purpose of turning over the oil and gas. For the installation of FPSO in deep water such as GoM, the development of a coupled dynamic analysis code for solving the large yaw motion and the interaction problem of multiple-body system becomes indispensable.

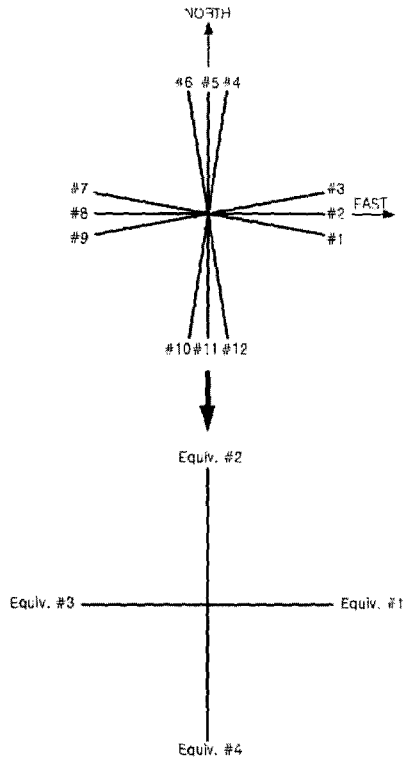

Figure 2: Configuration of the arrangement of the mooring line groups

Here, the program to investigate the multiple body interaction effects between a floating platform and a shuttle tanker considering the coupled effect with mooring lines and risers was developed and applied to an FPSO-FPSO model and an FPSO-shuttle tanker model for the verification.

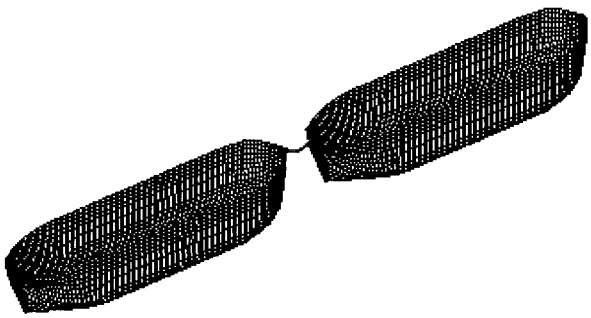

(a) Tandem arrangement

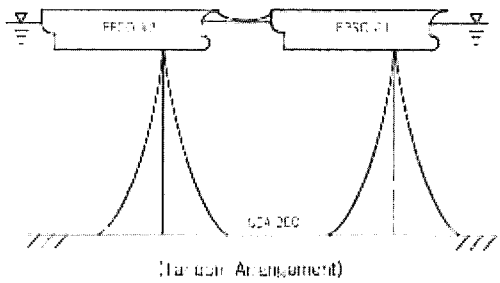

(b) Two-body model of FPSO-FPSO

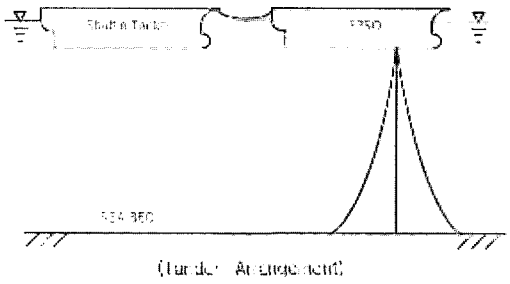

(c) Two-body model of FPSO and Shuttle tanker

Figure 3: Configuration of a two-body model and the mooring system

2 Background

The aspects of the hydrodynamic characteristics of the multiple-body structure combined with a barge and a mini TLP were studied by Teigen(2000). He compared the hydrodynamic coefficients of the multiple-body and the single-body and also conducted the convergence tests according to the mesh size of the multiple body. Using a three-dimensional source technique, Inoue et al(2001) solved the drift force for a multiple-body system of the FPSO-LNG carrier in parallel arrangement with zero forward speed waves. For a multi-body system with a side-by-side mooring of an FPSO and an LNG carrier, a linear potential solver was developed by Huijsmans(2001), and the mean and low-frequency wave drift forces were calculated by using it. For the same model, Buchner et al

(2001) conducted the numerical simulation for the prediction of hydrodynamic responses of an LNG FPSO with alongside moored an LNG carrier. The hydrodynamic interaction of forces and motions of the floating multiple-body was investigated using the WAMIT program (Lee 1999) and the higher-order boundary element method (Choi et al 2002).

The main objective of this research is to develop a numerical program to analyze the hydrodynamic interaction responses of multiple bodies, mooring lines and risers coupled with each other using the hydrodynamic coefficients calculated by WAMIT (Lee 1999) considering the interaction effects of the multiple-body. The hydrodynamic interaction analysis results with WAMIT and the conversion of the wind and current force data (OCIMF 1994) have to be prepared in advance to perform the coupled dynamic analysis program for considering the weathervaning motion and the inertaction effect of the ship-shaped multiple-body system(FPSO, LNG carrier etc). Two numerical experiments are performed to prove the validity of the newly developed program with the same models as Buchner's model (2001) and Choi's model (2002) for a comparative study. The former has the characteristics to deal with the close proximity problem of a side-by-side off-loading system. The latter took two same sized vessels of an FPSO and a shuttle tanker to tackle the problems of both cases of the side-by-side system and the tandem system, and used the higher-order boundary element method (HOBEM) while the constant panel method (CPM) was used in WAMIT. In this study, the coupled dynamic analysis scheme adopted for the program WINPOST-MULT was proved as the robust tool for analyzing the interaction problem of the multiple-body floating structures.

Dynamics of the floating platform

The wave loads and dynamic responses of floating structures are discussed. First, linear and second-order wave theories are reviewed in the consideration of the free surface boundary value problem, and then the boundary element method is applied as one of the solution schemes for the free surface boundary value problem. Next, Morison's equation and the wave drift damping are considered. Finally, the multiple-body interaction of fluid is reviewed, and then the dynamic motions for single body and multiple body systems of the floating structure are described, sequentially.

$$\nabla u = 0 \tag{1}$$

where,

$$\frac{\partial \Phi}{\partial z} = 0 \qquad \text{at} \qquad z = -d \tag{2}$$

$$\frac{\partial \Phi}{\partial t} + \frac{1}{2}\left(\nabla\Phi \cdot \nabla\Phi\right) + gz = 0 \qquad \text{at} \qquad z = -\eta \tag{3}$$

With the boundary conditions of equation (2) and (3), the perturbation formulation of the BVP with the first- and second-order parameters can give the first-order solution and the second-order solution.

Multiple body interaction of fluid

The boundary value problem of the multiple body interaction of fluid is explained that the effects of the incident potential and the scattered potential on the main body and the adjacent body are investigated. For the single body system, the radiation potential and the incident potential are obtained as described in the above sections. The diffraction problem for the isolated body can be defined by the incident potential as follows:

$$\frac{\partial \phi_7^I}{\partial n} = -\frac{\partial \phi_I}{\partial n} \quad \text{on} \quad S_I \tag{4}$$

$$\frac{\partial \phi_7^{II}}{\partial n} = -\frac{\partial \phi_I}{\partial n} \quad \text{on} \quad S_{II} \tag{5}$$

where S_I, S_{II} denotes the wetted surface of the isolated body I and II, respectively, ϕ_7, ϕ_7 denotes the scattered potential to the isolated body I and II, respectively, and ϕ_I represents the incident wave potential of the isolated body.

The boundary-value equation and the boundary condition for each body of the interaction problem is defined in the form of the radiation/scatter potential and the derivative as follows:

Interaction problem – radiation/scatter from *I* near *II*:

$$\frac{\partial \hat{\phi}_j^I}{\partial n} = -\frac{\partial \phi_j^I}{\partial n} \quad \text{on} \quad S_I \left(j = 1,2,\ldots,7\right) \tag{6}$$

$$\frac{\partial \hat{\phi}_j^I}{\partial n} = 0 \quad \text{on} \quad S_{II} \left(j = 1,2,\ldots,7\right) \tag{7}$$

Interaction problem – radiation/scatter from *II* near *I*:

$$\frac{\partial \hat{\phi}_j^{II}}{\partial n} = -\frac{\partial \phi_j^{II}}{\partial n} \quad \text{on} \quad S_{II} \left(j = 1,2,\ldots,7\right) \tag{8}$$

$$\frac{\partial \hat{\phi}_j^{II}}{\partial n} = 0 \quad \text{on} \quad S_I \left(j = 1,2,\ldots,7\right) \tag{9}$$

where $\hat{\phi}_j^{I,II}$ denotes the interaction potential affected by radiation/scatter potential from the body I to the body II, and vice versa, respectively. The potential when $j = 7$ means the scatter term. If the first-order radiation/scatter potential is used when the above BVP is solved, the resultant potential would be the first-order interaction potential, while the second-order radiation/scatter potential leads the second-order interaction potential.

Single body motion

The equilibrium equation using Newton's second law called the momentum equation for the floating structure can be given as:

$$\mathbf{M}\frac{d^2\mathbf{x}_{cg}}{dt^2} = \mathbf{f} \tag{10}$$

$$\mathbf{I}\frac{d\varphi}{dt} + \varphi \times \left(\mathbf{I}\varphi\right) = \mathbf{m} \tag{11}$$

where $\mathbf{M}$ is the mass of the floating structure, $\mathbf{x}$ is the coordinates of the center of gravity of the floating body, $\mathbf{I}$ is the moment of inertia, and φ is the angular velocity, $\mathbf{f}$ and $\mathbf{m}$ are the external force and moment. The second term of the left-hand side of the equation (11) and the relative angular motion of the body to the wave motion are nonlinear. If the rotation is assumed to be small, the equation (10) becomes a linear equation as follows:

$$\mathbf{M}\ddot{\varsigma} = \mathbf{F}(t) \tag{12}$$

where $\ddot{\varsigma}$ is the normal acceleration of body motion, $\mathbf{M}$ is the 6×6 body mass matrix and $\mathbf{F}(t)$is the external force vector. In the time domain, the above equation is expanded as:

$$\left[\mathbf{M}+\mathbf{M}^{a}(\infty)\right]\ddot{\varsigma}+\mathbf{K}\varsigma = \mathbf{F}_{I}(t)+\mathbf{F}_{c}(\dot{\varsigma},t)+\mathbf{F}_{m}(\dot{\varsigma},t) \tag{13}$$

where $\mathbf{F}_I$ is the wave exciting force induced by the incident potential and the diffraction potential, $\mathbf{F}_m$ is the force by Morison's equation, and $\dot{\varsigma}$ and $\ddot{\varsigma}$ are the velocity and acceleration of the body, respectively. $\mathbf{M}^a(\infty)$ is a constant, equivalent added mass of the body at the infinite frequency and can be expressed by:

$$\mathbf{M}^{a}(\infty) = \mathbf{M}^{a}(\omega) - \int_{0}^{\infty} R(t)\cos\omega t dt \tag{14}$$

where $\mathbf{F}_c$ is the current force, and can be defined as follows:

$$\mathbf{F}_{c}(\dot{\varsigma},t) = -\int_{-\infty}^{t}\mathbf{R}(t-\tau)\dot{\varsigma}d\tau \tag{15}$$

As shown in the above equation, the current force, $\mathbf{F}_c$, can be obtained in the form of the convolution integration of the retardation function multiplied by the body velocity. The Morison's equation is given by

$$F_{m} = C_{m}\rho V\dot{u}_{n} - C_{a}\rho V\ddot{\varsigma}_{n} + \frac{1}{2}\rho C_{D}D_{S}\left(u_{n}-\dot{\zeta}_{n}\right)\left|u_{n}-\dot{\zeta}_{n}\right| \tag{16}$$

where $V = \pi D^2/4$ is the volume per unit length of the structure, C_m is the inertia coefficient, C_a is the added mass coefficient, C_D is the drag coefficient, D_S is the breadth or diameter of the structure body, u_n and $\dot{u}_n$ are the velocity and acceleration of the fluid, respectively, and $\dot{\zeta}_n$ and $\ddot{\varsigma}_n$ are the normal velocity and acceleration of the body, respectively.

Multiple body motion

For the multiple body system, the number of the degrees of freedom of the mass matrix, the body motion vector and the force vector in the equation (12) are changed to $6N\times6N$, $6N$ and $6N$, of which N is the number of bodies. In the total system equation (13), the matrix sizes are extended accordingly. For the formulation of motion, the local coordinate system is used for each body. After forming the equation of motion for each body, the coordinate transformation is needed. Finally, the total equation of motion in the global coordinate system is assembled for the combined system. The hydrodynamic coefficients are pre-made in consideration of the fluid-interaction terms influenced on each body by using WAMIT. The hydrodynamic coefficients are solved in the sequence as follows:

1) The radiation/diffraction problem for each body in isolation
2) The interaction problem resulting from radiation/scatter from body I in the presence of body II, and radiation/scatter from body II in the presence of body I.

where body I and II represent one pair of bodies which interacts hydro-dynamically with each other. If there are several bodies, the two-body problem should be addressed for each unique pair of bodies. The boundary-value problem is formed differently due to the different kinematic boundary condition on the immersed surface of bodies, but other boundary conditions for the bodies are the same as those in the isolated body.

The boundary–value problem of fluid interaction is solved using the equation (6) to (9) in the form of an excitation force coefficient as follows:

$$C_j^{I,I} = -\int_{S_I} a\hat{\phi}_7^I n_j dS, \tag{17}$$

$$C_j^{II,II} = -\int_{S_I} a\hat{\phi}_7^{II} n_j dS, \tag{18}$$

$$C_j^{I,II} = -\int_{S_I} a(\hat{\phi}_7^{II} + \phi_7^{II}) n_j dS, \tag{19}$$

$$C_j^{II,I} = -\int_{S_{II}} a(\hat{\phi}_7^{I} + \phi_7^{I}) n_j dS, \tag{20}$$

$$(j = 1,2,\ldots,6)$$

where the superscript I and II represent the body I and II. If the coefficients are written in the form of equation (14), the hydrodynamic coefficients are obtained by:

$$M^{a^{I,I}}(\infty) = -\int_{S_I} \hat{\phi}_j^I n_i dS \tag{21}$$

$$M^{a^{II,II}}(\infty) = -\int_{S_{II}} \hat{\phi}_j^{II} n_i dS \tag{22}$$

$$M^{a^{I,II}}(\infty) = -\int_{S_I} (\hat{\phi}_j^{II} + \hat{\phi}_j^{II}) n_i dS \tag{23}$$

$$M^{a^{II,I}}(\infty) = -\int_{S_{II}} (\hat{\phi}_j^{I} + \hat{\phi}_j^{I}) n_i dS \tag{24}$$

$$(i, j = 1,2,\cdots,6)$$

Then, for the two-body problem, the equation (21) to equation (24) are replaced for the equation (13), and the other matrices contain the terms for two bodies. Thus,

$$\mathbf{M} = \begin{bmatrix} \mathbf{M}^I & 0 \\ 0 & \mathbf{M}^{II} \end{bmatrix}, \tag{25}$$

$$\mathbf{K} = \begin{bmatrix} \mathbf{K}^{I,I} & \mathbf{K}^{I,II} \\ \mathbf{K}^{II,I} & \mathbf{K}^{II,II} \end{bmatrix}, \tag{26}$$

$$\mathbf{F}_I = \begin{bmatrix} \mathbf{F}_I^{II} \\ \mathbf{F}_I^{II} \end{bmatrix}, \tag{27}$$

$$\mathbf{F}_C = \begin{bmatrix} \mathbf{F}_C^{I} \\ \mathbf{F}_C^{II} \end{bmatrix}, \tag{28}$$

$$\mathbf{F}_m = \begin{bmatrix} \mathbf{F}_m^{I} \\ \mathbf{F}_m^{II} \end{bmatrix}, \tag{29}$$

The total equation of motion of the system has the same form of equation (12), but for the N-body with 6 DOF for each body, the matrices are of the size of $6N \times 6N$

Table 1: Main particulars of the turret moored FPSO

Description	Unit	Quantity
Pretension	*kN*	1,201
Number of lines		4*3
Degrees between 3 lines	*deg*	5
Length of mooring line	*m*	2,087.9
Radius of location of chain stoppers on turn table	*m*	7.0
Segment 1 (ground position): chain		
Length at anchor point	*m*	914.4
Diameter	*mm*	88.9
Weight in air	*kg/m*	164.9
Weight in water	*kg/m*	143.4
Stiffness, AE	*kN*	794,841
Mean breaking load, MBL	*kN*	6,515
Segment 2: chain		
Length	*m*	1127.8
Diameter	*mm*	107.9
Weight in air	*kg/m*	42.0
Weight in water	*kg/m*	35.7
Stiffness, AE	*kN*	690,168
Mean breaking load, MBL	*kN*	6,421
Segment 3 (hang-off position): chain		
Length	*m*	45.7
Diameter	*mm*	88.9
Weight in air	*kg/m*	164.9
Weight in water	*kg/m*	143.4
Stiffness, AE	*kN*	794,841
Mean breaking load, MBL	*kN*	6,515

Table 2: Main particulars of the mooring systems

Description	Symbol	Unit	Quantity
Production level		*bpd*	120,000
Storage		*bbls*	1,440,000
Vessel size		*kDWT*	200
Length between perpendicular	Lpp	*m*	310.0
Breadth	B	*m*	47.17
Depth	H	*m*	28.04
Draft (in full load)	T	*m*	18.09
Diaplacement (in full load)		*MT*	240,869
Length-beam ratio	L/B		6.57
Beam-draft ratio	B/T		2.5
Block coefficient	Cb		0.85
Center of buoyancy forward section 10	FB	*m*	6.6
Water plane area	A	m^2	13,400
Water plane coefficient	Cw		0.9164
Center of water plane area forward section 10	FA	*m*	1.0
Center of gravity above keel	KG	*m*	13.32
Transverse metacentric height	MGt	*m*	5.78
Longitudinal metacentric height	MGl	*m*	403.83
Roll raius of gyration in air	R_{xx}	*m*	14.77
Pitch raius of gyration in air	R_{yy}	*m*	77.47
Yaw radius of gyration in air	R_{zz}	*m*	79.30
Frontal wind area	Af	m^2	1,012
Transverse wind area	Ab	m^2	3,772
Turret in center line behind Fpp (20.5 % Lpp)	Xtur	*m*	63.55
Turret elevation below tanker base	Ztur	*m*	1.52
Turret diameter		*m*	15.85

Table 3: Environmental conditions (100-year storm condition at GOM)

Description	Unit	Quantity
Wave		
Significant wave height, Hs	*m*	2.70
Peak period, Tp	*sec*	16.5
Wave spectrum	*JONSWAP (γ=6.0)*	
Direction	*deg*	180 [1)]
Wind		
Velocity	*m/s*	5.0 m/s @ 10m
Spectrum	*API RP 2A-WSD*	
Direction	*deg*	210 [1)]
Current		
Profile		
at free surface (0 m)	*m/s*	0.150
at 60.96 m	*m/s*	0.150
at 91.44 m	*m/s*	0.050
on the sea bottom	*m/s*	0.050
Direction	*deg*	150 [1)]

Remark: 1) The angle is measured counterclockwise from the x-axis (the East).

Table 4: Environmental conditions (west Africa sea condition)

Description	Unit	Quantity
Wave		
Significant wave height, Hs	*m*	12.19
Peak period, Tp	*sec*	14.0
Wave spectrum	*JONSWAP (γ=2.5)*	
Direction	*deg*	180 [1)]
Wind		
Velocity	*m/s*	41.12 m/s @ 10m
Spectrum	*API RP 2T*	
Direction	*deg*	210 [1)]
Current		
Profile		
at free surface (0 m)	*m/s*	1.0668
at 60.96 m	*m/s*	1.0668
at 91.44 m	*m/s*	0.0914
on the sea bottom	*m/s*	0.0914
Direction	*deg*	150 [1)]

Remark: 1) The angle is measured counterclockwise from the x-axis (the East).

3 Example of application

Objective

For the verification, an FPSO-FPSO in the 100-year storm condition in GOM (table 3) and an FPSO-Shuttle tanker in the environmental condition in West Africa sea (table 4) are taken as the multiple-body models for the verification of the program (WINPOST-MULT)

for the dynamic coupled analysis of the multiple-body floating platforms, and the results of the FPSO-FPSO model are compared with the exact solution using a two-mass-spring model. The simplified mass-spring model will give a compatible result to judge the validity of the multiple-body program. The two-body model is composed of an FPSO and a shuttle tanker. The conventional tandem moorings have been used for the multiple-body connections in many cases of the operation of offloading in the sea. For the multiple-body model of the FPSO-shuttle tanker, the tandem mooring is considered to investigate the interaction effect. The effect of the hawser to connect two structures is also specified. The both models with a hawser and without a hawser are made and analyzed.

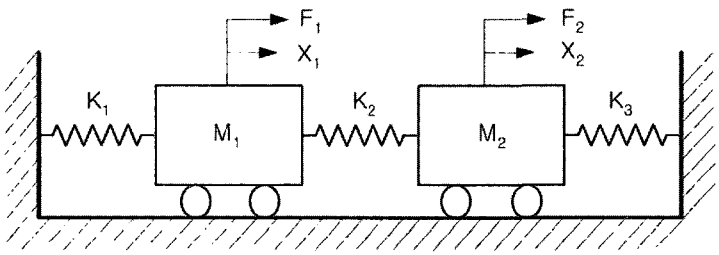

Figure 4: Two-mass-spring model

Table 5: The system parameters for two-mass -spring model

	Mean	Min.	Max.	RMS
Mass #1	-15.47	-38.99	11.71	14.46
Mass #2	-15.45	-42.97	8.55	14.08

The hydrodynamic interaction characteristics for the tandem-moored vessels are calculated in regular waves at several frequencies by using WAMIT. The body motions and line tensions are mainly reviewed with the numerical calculations performed by WINPOST-MULT, the dynamic coupled analysis program for multiple-body platforms.

Table 6: Analysis results of mass-spring model: displacement at mass #1 and #2 (unit: m)

ITEM	Symbol	Unit	Magnitude
Added mass	m_a	*kg*	1.466E+07
FPSO weight in mass	m	*kg*	2.397E+08
Mass of FPSO #1	M_1	*kg*	2.543E+08
Mass of FPSO #2	M_2	*kg*	2.543E+08
Stiffness of mooring #1	K_1	*N/m*	2.389E+05
Stiffness of hawser	K_2	*N/m*	1.868E+03
Stiffness of mooring #2	K_3	*N/m*	2.389E+05
Natural period (Mode #1)		*sec*	16.34
(Mode #2)		*sec*	205.02

Results and discussions

In table 5, the statistics of the analysis results for the mass-spring model is shown. The analysis results for the FPSO and FPSO model are summarized in table 6 and 7. The two tables show that the statistical results are well matched with each other. In figure 5 (a)~(d),

the displacements in x-direction (surge motion) by the time simulation analyses for the mass-spring model and the FPSO and FPSO model when the mooring is in tandem arrangement are depicted. The hawser stiffness used for this analysis was 1/100th of the mooring stiffness, and the top tension of the hawser was taken as 1/10th of the mooring line tension. The surge motion amplitude for each case is very similar, so that the validity of the program WINPOST-MULT for the two-body analysis with one hawser is proved. However, whether the interaction effect is considered or not affects the shape and the phase difference between surge motions of two bodies in the time simulation.

Table 7: Summary of the analysis results for two body FPSO+FPSO

		Single FPSO	FPSO+FPSO[1)]											
			w/o interaction				with interaction (by iteration method)				with interaction (by combined method)			
			w/o hawser		with hawser		w/o hawser		with hawser		w/o hawser		with hawser	
			FPSO 1	FPSO 2	FPSO 1	FPSO 2	FPSO 1	FPSO 2	FPSO 1	FPSO 2	FPSO 1	FPSO 2	FPSO 1	FPSO 2
Body Motion														
surge (m)	mean	**-14.63**	-14.19	-13.98	-13.70	-13.36	-13.86	-10.95	-14.97	-7.89	-14.72	-10.34	-13.24	-9.32
	min.	**-35.57**	-34.51	-33.36	-37.45	-37.55	-33.15	-20.09	-34.78	-22.53	-34.38	-24.64	-36.30	-21.49
	max.	**3.07**	3.55	3.25	7.89	7.50	-1.37	-1.98	3.63	4.07	0.50	-2.18	6.24	1.81
	rms.	**8.01**	8.55	8.59	9.23	9.20	7.25	4.06	8.05	5.93	7.27	4.19	8.06	4.40
sway (m)	mean	**4.41**	4.59	4.19	3.65	4.06	3.76	4.07	1.81	1.43	4.56	3.34	3.23	3.51
	min.	**-0.91**	-0.98	-0.56	-1.13	-1.48	-2.35	-1.73	-3.03	-5.53	-2.84	-3.13	-3.09	-3.53
	max.	**12.59**	13.93	10.74	8.77	10.88	11.43	12.23	7.04	10.94	13.89	9.82	11.61	14.41
	rms.	**2.68**	2.87	2.47	1.42	1.88	2.81	3.33	2.17	3.61	2.98	2.96	2.11	3.01
heave (m)	mean	**-1.32**	-1.31	-1.30	-1.27	-1.28	-1.18	-0.71	-1.19	-0.67	-1.29	-0.69	-1.24	-0.70
	min.	**-9.58**	-10.30	-9.95	-9.44	-9.65	-8.68	-3.29	-8.26	-3.22	-9.43	-3.41	-10.42	-3.83
	max.	**5.79**	6.39	6.37	5.52	5.72	5.50	1.25	5.26	1.37	5.91	1.52	6.49	2.01
	rms.	**2.60**	2.57	2.54	2.47	2.51	2.32	0.72	2.28	0.62	2.55	0.67	2.43	0.72
roll (deg)	mean	**0.00**	-0.01	-0.01	0.00	0.00	-0.01	-0.07	0.04	0.02	-0.03	0.00	0.00	-0.04
	min.	**-4.87**	-4.54	-5.35	-2.97	-5.15	-5.93	-3.15	-1.38	-1.83	-8.11	-3.12	-4.83	-4.09
	max.	**4.70**	4.36	5.66	2.95	5.08	6.02	2.91	1.54	1.57	7.53	2.85	4.67	3.20
	rms.	**1.50**	1.45	1.34	0.90	1.34	1.76	0.83	0.37	0.53	2.42	0.66	1.38	0.82
pitch (deg)	mean	**0.45**	0.45	0.45	0.43	0.44	0.41	0.25	0.40	0.23	0.44	0.24	0.42	0.24
	min.	**-3.12**	-3.44	-3.55	-3.36	-3.45	-2.82	-0.79	-2.89	-0.78	-3.09	-0.87	-3.40	-0.97
	max.	**4.93**	5.48	5.41	5.08	5.18	4.47	1.18	4.20	1.15	4.87	1.23	5.25	1.44
	rms.	**1.45**	1.44	1.42	1.39	1.41	1.28	0.31	1.28	0.26	1.40	0.29	1.34	0.31
yaw (deg)	mean	**9.52**	9.85	8.65	6.56	8.46	12.92	18.75	1.82	12.48	11.47	18.59	9.33	16.67
	min.	**0.80**	3.79	0.47	2.53	2.45	3.65	10.73	-2.37	5.61	3.52	14.83	0.62	8.24
	max.	**17.85**	17.23	16.14	11.49	13.57	21.87	26.46	5.53	16.86	20.19	21.72	16.77	23.20
	rms.	**4.08**	2.82	3.61	1.56	2.29	5.18	4.07	1.99	2.41	4.26	1.68	3.43	2.75
Line Tension														
Mooring line #1 (kN)	mean	**6,399**	6,349	6,313	6,271	6,216	6,285	5,873	6,477	5,413	6,416	5,780	6,193	5,619
	min.	**3,516**	3,480	3,373	3,041	3,025	4,001	4,369	3,543	3,634	3,859	4,312	3,330	3,802
	max.	**10,570**	10,430	9,757	10,480	10,490	10,110	7,601	10,080	7,932	10,330	8,263	10,700	7,818
	rms.	**1,306**	1,377	1,373	1,470	1,466	1,167	654	1,297	927	1,184	673	1,291	701
Mooring line #2 (kN)	mean	**3,537**	3,506	3,553	3,617	3,565	3,621	3,642	3,872	3,994	3,512	3,728	3,679	3,710
	min.	**1,759**	1,884	2,098	2,286	2,033	2,102	2,455	2,805	2,631	1,788	2,604	1,989	2,237
	max.	**4,768**	4,889	4,968	4,783	4,734	4,685	4,672	5,350	5,098	5,040	4,784	4,923	4,792
	rms.	**488**	496	460	383	409	473	440	435	500	500	405	427	405
Mooring line #3 (kN)	mean	**2,585**	2,634	2,662	2,704	2,730	2,639	2,847	2,556	3,208	2,554	2,929	2,700	3,019
	min.	**570**	535	608	558	530	785	1,868	622	1,798	693	1,754	668	1,828
	max.	**4,853**	5,085	5,051	5,724	5,704	4,496	3,879	4,857	4,780	4,562	3,995	5,284	4,455
	rms.	**767**	866	878	913	920	677	417	766	669	709	431	815	484
Mooring line #4 (kN)	mean	**4,765**	4,809	4,751	4,667	4,728	4,701	4,796	4,411	4,419	4,803	4,691	4,609	4,711
	min.	**3,349**	3,193	3,194	3,326	3,345	3,384	3,697	2,887	3,404	2,937	3,625	3,328	3,677
	max.	**6,906**	7,073	6,613	6,224	6,704	6,747	6,335	5,550	5,900	7,231	5,956	6,580	6,598
	rms.	**561**	591	542	430	483	563	513	462	534	619	452	492	462
Riser (kN)	mean	**109,800**	109,800	108,700	107,300	108,100	102,900	75,360	103,700	73,270	110,500	73,870	106,400	74,360
	min.	**0**	0	0	0	0	0	0	0	0	0	0	0	0
	max.	**676,700**	724,600	721,900	655,700	671,900	663,300	255,100	638,900	254,800	703,200	274,300	734,500	316,400
	rms.	**132,300**	131,100	130,300	127,000	128,400	120,000	5,006	120,100	45,060	131,000	48,330	125,300	49,850
Hawser (kN)	mean					101				101				102
	min.					100				100				100
	max.					103				104				106
	rms.					0				1				1

Remarks: 1) Both FPSOs have 4 equivalent mooring lines and 1 equivalent central riser.

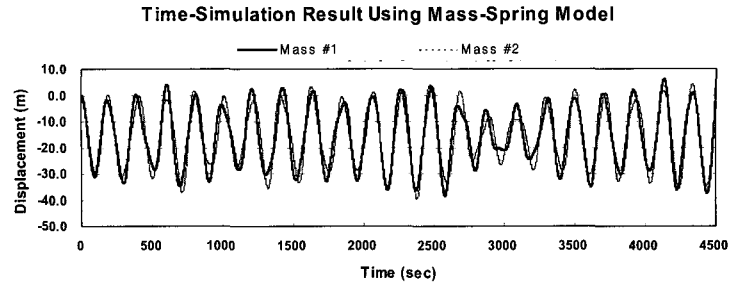

(a) Displacements by MATLAB

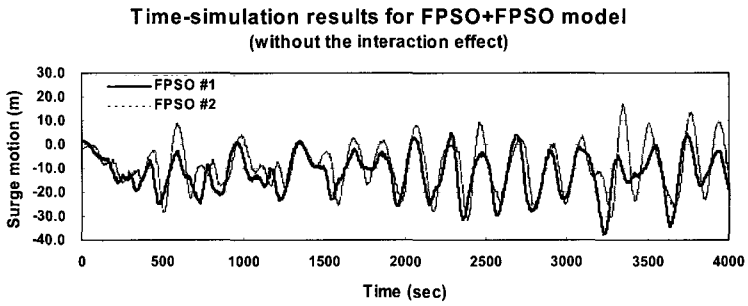

(b) w/o the interaction effect by PGM

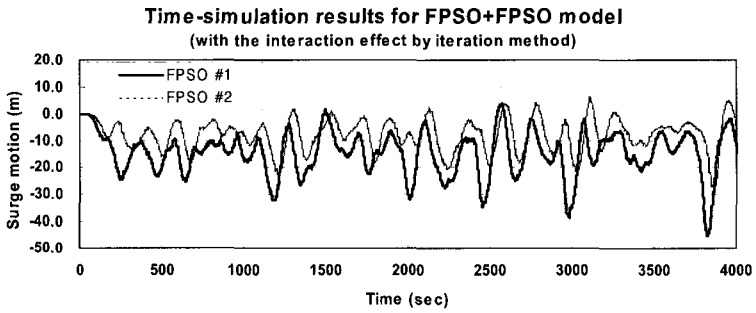

(c) w. inter. effect by I-method by PGM

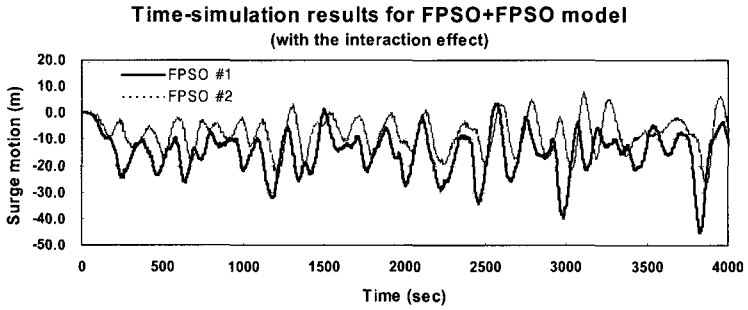

(d) w. inter. effect by C-method by PGM

Figure 5: The surge motion of FPSO- FPSO model by MATLAB and by WINPOST-MULT

Table 8: Summary of the analysis results for the two-body FPSO+shuttle tanker

		Single FPSO	FPSO+Shuttle Tanker[2)]					
			w/o interaction		with interaction by the iteration method		with interaction by the combined method	
			with hawser		with hawser		with hawser	
			FPSO	Shuttle	FPSO	Shuttle	FPSO	Shuttle
Body Motion								
surge (m)	mean	**-0.46**	-0.91	21.72	-0.67	16.86	-0.39	17.51
	min.	**-2.01**	-5.74	-6.13	-2.23	6.11	-1.52	8.14
	max.	**0.81**	1.81	54.15	0.80	33.16	0.41	24.26
	rms.	**0.51**	1.54	17.69	0.62	8.10	0.35	5.09
sway (m)	mean	**0.12**	0.03	-0.12	0.05	2.50	0.01	3.50
	min.	**-0.65**	-0.79	-8.57	-1.16	-2.59	-1.26	-2.81
	max.	**0.85**	0.84	5.44	1.38	8.74	1.41	9.25
	rms.	**0.28**	0.39	3.62	0.48	3.70	0.47	4.11
heave (m)	mean	**-0.60**	-0.60	0.77	-0.60	0.77	-0.60	0.77
	min.	**-1.58**	-1.48	-2.66	-1.40	-1.62	-1.44	-1.73
	max.	**0.43**	0.27	4.19	0.23	3.34	0.28	3.41
	rms.	**0.27**	0.26	1.15	0.27	0.86	0.26	0.87
roll (deg)	mean	**0.00**	0.00	0.00	0.00	0.00	0.00	0.00
	min.	**-0.47**	-0.26	-0.66	-0.11	-0.23	-0.32	-0.34
	max.	**0.51**	0.28	0.65	0.10	0.23	0.33	0.34
	rms.	**0.14**	0.05	0.13	0.01	0.06	0.11	0.08
pitch (deg)	mean	**0.21**	0.21	-0.27	0.21	-0.27	0.21	-0.27
	min.	**-0.51**	-0.39	-1.66	-0.36	-1.28	-0.33	-1.31
	max.	**0.97**	0.84	1.16	0.81	0.69	0.79	0.73
	rms.	**0.20**	0.20	0.48	0.20	0.34	0.19	0.35
yaw (deg)	mean	**0.98**	0.48	3.20	-0.38	5.02	-5.71	10.62
	min.	**-1.21**	-2.99	-2.46	-2.56	0.62	-7.67	4.50
	max.	**2.52**	2.72	7.54	2.34	10.17	-0.07	14.75
	rms.	**1.11**	0.16	3.11	1.13	2.69	1.68	2.84
Line Tension								
Mooring line #1 (kN)	mean	**4,268**	4,339		4,298		4,257	
	min.	**4,086**	3,944		4,094		4,122	
	max.	**4,487**	5,050		4,509		4,428	
	rms.	**74**	232		89		51	
Mooring line #2 (kN)	mean	**4,174**	4,187		4,184		4,189	
	min.	**3,974**	4,018		3,946		3,965	
	max.	**4,350**	4,375		4,408		4,397	
	rms.	**57**	67		78		75	
Mooring line #3 (kN)	mean	**4,115**	4,051		4,086		4,126	
	min.	**3,811**	3,374		3,779		3,918	
	max.	**4,367**	4,508		4,375		4,353	
	rms.	**93**	225		104		74	
Mooring line #4 (kN)	mean	**4,210**	4,197		4,200		4,195	
	min.	**4,041**	4,019		3,967		3,991	
	max.	**4,422**	4,353		4,449		4,433	
	rms.	**54**	67		78		78	
Riser (kN)	mean	**69,550**	69,530		69,490		69,560	
	min.	**0**	0		0		0	
	max.	**164,900**	150,600		146,600		151,300	
	rms.	**24,730**	24,170		24,410		23,730	
Hawser (kN)	mean		254		119		79	
	min.		5		6		6	
	max.		844		296		252	
	rms.		254		86		77	

2) The loading condition is changed for this calculation, which is intended to investigate the difference with the results by three methods in a mild loading condition (West Africa sea condition).The wind velocity is 10 m/s at 10 m height, the current speed is 0.15 m/s at free surface, and the wave has Hs of 2.7 m, Tp of 16.5 sec, and gamma of 6.0.

In table 8, the analysis cases for the two-body model of an FPSO and a shuttle tanker are summarized for three different cases. The hawser stiffness used for this analysis was 1/1000th of the mooring stiffness, and the top tension of the hawser was taken as 1/10th of the mooring line tension. In the case of "no interaction", the hydrodynamic coefficients induced by wave, the body stiffness matrix and mass matrix have only the terms for the single body, and the interaction terms are set to zero. That means, in this case, the interaction effect between two vessels of the fluid and the structures is not considered. In the case of the "with the interaction effect by iteration method" for the two-body model,

the self-coupling terms in the hydrodynamic coefficients, and the multiple-body stiffness matrix and the multiple-body mass matrix are only considered. In this method, the off-diagonal interaction terms coupled with other bodies are not considered. Thus, the iteration scheme is used to get the converged solution bounded within a pre-set error norm. In the case of the "with the interaction effect by the combined method", the fully coupled terms with multiple bodies are used for the analysis. The purpose of this study is to compare the analyzed results by the developed program with the results produced by the methods used in the industry. The program WINPOST-MULT has the kind function of performing the above three cases by handling the system matrix or the hydrodynamic coefficient matrices. In table 8, to review the results of all cases can make some clues drawn about the hawser connection effect and the hydrodynamic interaction effect between two bodies. In all motions at the rear side vessel, the interaction and hawser effects are clearly illustrated. The time simulation results are shown for the purpose of comparison in figure 6. In the two-body model of the FPSO and shuttle tanker, the analysis results for the case of "with interaction by the iteration method" give medium values among the results for the cases of "with no interaction" and "with interaction by the combined method". It means that it is significant to consider the fully coupled interaction effect for the two-body analysis.

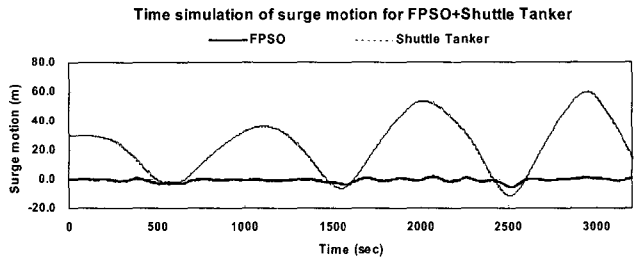

(a) w/o interaction effect

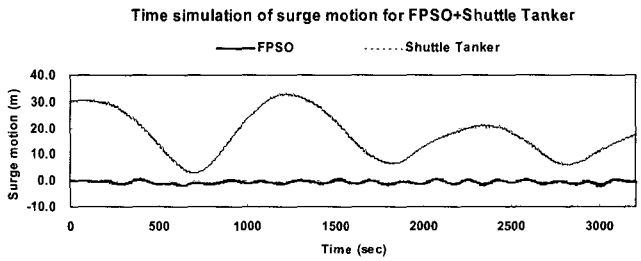

(b) with interaction effect by I-method

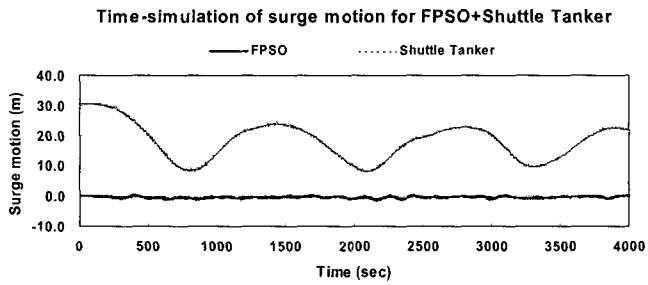

(c) with interaction effect by C-method

Figure 6: The time simulation results of the FPSO and shuttle tanker model

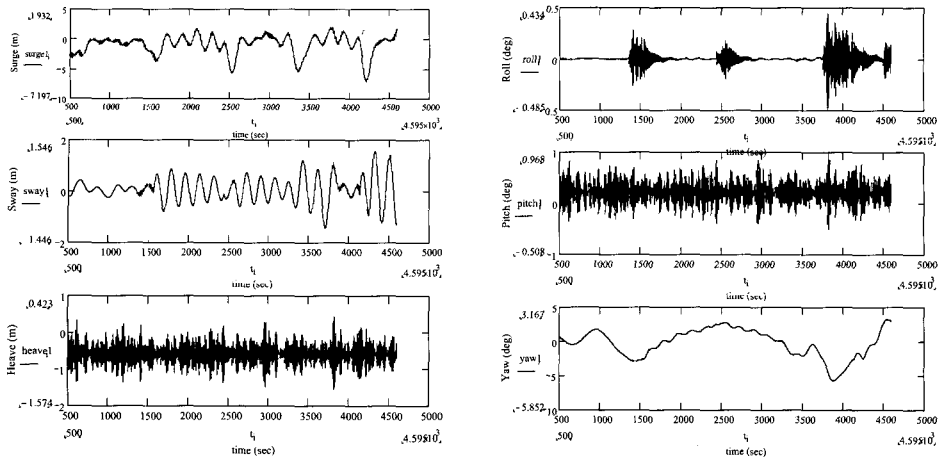

(a) w/o interaction effect

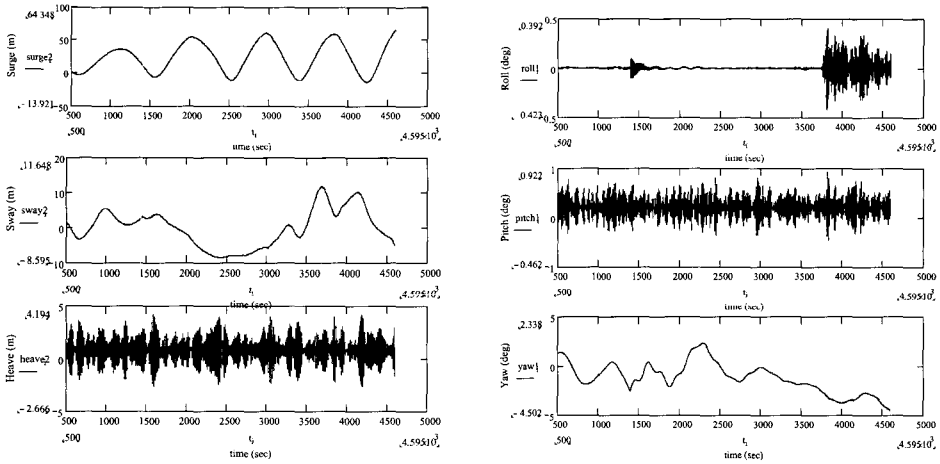

(b) with interaction effect by iteration method

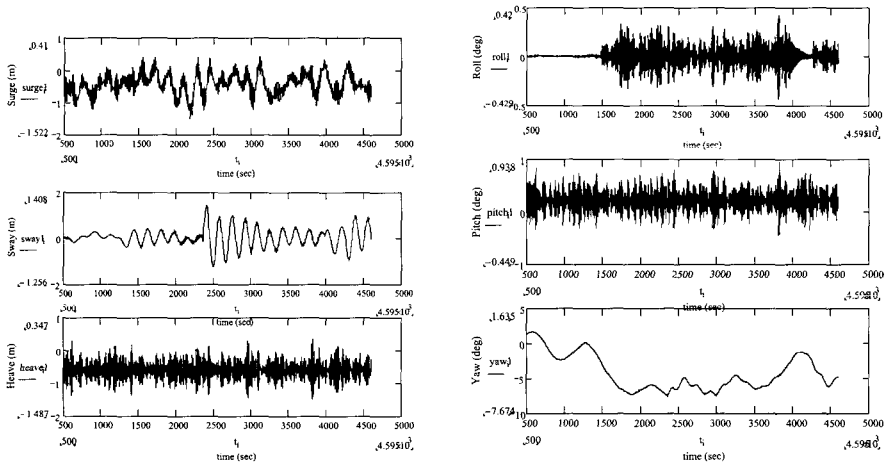

(c) with interaction effect by combined method

Figure 7: Time simulation for the two body model of the FPSO and shuttle tanker in tandem arrangement by different methods

In the figures 7, the time histories and the motion amplitude spectra are shown for all analysis cases. To review the motion amplitude spectrum for each case, the vessels have almost the same characteristics in their dynamic behaviors.

4 Conclusion

The hydrodynamic interaction effects and the coupling effects of the hull/mooring/riser /hawser with the multiple body system are investigated by several numerical simulations. Two models, which are an FPSO-FPSO and an FPSO-shuttle tanker, are taken as the multiple body systems, and the tandem mooring is considered. The distance effects on motions and drift forces of two vessels have already been reviewed by Hong (2002). The coupling and interaction effects are studied using the above two kinds of two-body models.

The analysis results for the FPSO and FPSO model and the mass-spring model show the validity of the program WINPOST-MULT. The comparative study of an FPSO and a shuttle tanker illustrates the importance of the interaction effect between bodies for the interaction problem of the multiple floating platforms. In addition, it reveals that the combined method is more reasonable approach than the iteration method.

References

Arcandra, T. 2001. Hull/Mooring/Riser Coupled Dynamic Analysis of a Deepwater Floating Platform with Polyester Lines. Ph.D. Dissertation, Texas A&M University.

Buchner, B, A. van Dijk and J.J. de Wilde. 2001. Numerical multiple-body simulations of side-by-side moored to an FPSO. Proc. 11th Int. Offshore and Polar Eng. Conference, ISOPE, **1**, 343-353.

Choi, Y.R. and S.Y. Hong. 2002. An analysis of hydrodynamic interaction of floating multi-body using higher-order boundary element method. Proc. 12th Int. Offshore and Polar Eng. Conference, ISOPE, **3**, 303-308.

Garrett, D.L. 1982. Dynamic analysis of slender rods. J. Energy Resources Technology, Trans. of ASME, **104**, 302-307.

Garrison, C.J. 2000. An Efficient time-domain analysis of very large multi-body floating structures. Proc. 10th Int. Offshore and Polar Eng. Conference, ISOPE, **1**, 65-71.

Huijsmans, R.H.M., J.A. Pinkster and J.J. de Wilde. 2001. Diffraction and radiation of waves around side-by-side moored vessels. Proc. 11th Int. Offshore and Polar Eng. Conference, ISOPE, **1**, 406-412.

Hong, S.Y., J.H. Kim, H.J. Kim and Y.R. Choi. 2002. Experimental study on behavior of tandem and side-by side moored vessels. Proc. 12th Int. Offshore and Polar Eng. Conference, ISOPE, **3**, 841-847.

Inoue, Y. and M.R. Islam. 2001. Effect of viscous roll damping on drift forces of multi-body floating system in waves. Proc. 11th Int. Offshore and Polar Eng. Conference, ISOPE, **1**, 279-285.

Kim, M.H. 1992. WINPOST V3.0 Users Manual. Dept. of Ocean Engineering, Texas A&M University.

Kim, M.H., T. Arcandra and Y.B. Kim. 2001a. Validability of spar motion analysis against various design methodologies/parameters. Proc. 20th Offshore Mechanics and Arctic Eng. Conference, OMAE01-OFT1063 [CD-ROM].

Kim, M.H., T. Arcandra and Y.B. Kim. 2001b. Validability of TLP motion analysis against various design methodologies/parameters. Proc. 12th Int. Offshore and Polar Eng.

Conference, ISOPE, **3**, 465-473.

Kim, M.H. and Z. Ran. 1994. Response of an articulated tower in waves and currents. International J. Offshore and Polar Engineering, **4**, **4**, 298-231.

Kim, M.H., Z. Ran and W. Zheng. 1999. Hull/mooring/riser coupled dynamic analysis of a truss spar in time-domain. Proc. 9th Int. Offshore and Polar Eng. Conference, ISOPE, Brest, France, **1**, 301-308.

Kim, M.H. and D.K.P. Yue. 1989a. The complete second-order diffraction solution for an axisymmetric body. Part 1. monochromatic incident waves. J. Fluid Mechanics, **200**, 235-264.

Kim, M.H. and D.K.P. Yue. 1989b. The complete Second-order diffraction solution for an axisymmetric body. Part 2. bichromatic incident waves. J. Fluid Mechanics, **211**, 557-593.

Lee, C.H. 1999. WAMIT User Manual. Dept. of Ocean Engineering, Massachusetts Institute of Technology, Cambridge, M.A.

Ma, W., M.Y. Lee, J. Zou and E. Huang. 2000. Deep water nonlinear coupled analysis tool. Proc. Offshore Technology Conference, OTC 12085 [CD-ROM].

OCIMF 1994 Prediction of Wind and Current Loads on VLCCs. 2nd Edition, Witherby & Co. Ltd, London, England.

Pauling, J.R. and W.C. Webster. 1986. A consistent large-amplitude analysis of the coupled response of TLP and tendon system. Proc. 5th OMAE Conf., **3**, 126-133.

Ran, Z. and M.H. Kim. 1997. Nonlinear coupled responses of a tethered spar platform in waves. International J. Offshore and Polar Engineering, **7**, **2**, 27-34.

Ran, Z., M.H. Kim and W. Zheng. 1999. Coupled dynamic analysis of a moored spar in random waves and currents (time-domain versus frequency-domain analysis). J. Offshore Mechanics and Arctic Engineering, **121**, **2**, 194-200.

Teigen, P. and K. Trulsen. 2001. Numerical investigation of nonlinear wave effects around multiple cylinders. Proc. 11th Int. Offshore and Polar Eng. Conference, ISOPE, **3**, 369-378.

Wichers, J.E.W. 1988. A Simulation Model for a Single Point Moored Tanker. Ph.D. Dissertation, Delft University of Technology, Delft, The Netherlands.